Positron Scattering from Atoms and Molecules at Low Energies

S. J. Gilbert, R. G. Greaves,* and C. M. Surko

Department of Physics, University of California, San Diego, California 92093-0319
(Received 26 January 1999)

Elastic and inelastic scattering of positrons by atoms and molecules are studied experimentally in a new range of positron energies, using a novel technique involving a magnetized beam of cold positrons. Differential cross-section measurements are presented for Ar and Kr at energies from 0.4 to 2.0 eV, and they compare well with theoretical predictions. The first low-energy measurements of the vibrational excitation of molecules by positrons is presented (i.e., CF_4 at energies from 0.2 to 1 eV), and comparison with electron scattering data is discussed. [S0031-9007(99)09412-0]

PACS numbers: 34.85.+x, 34.50.Ez, 41.75.Fr

Study of positron-matter interactions is an active area of research [1–7]. The simplest form of such interactions are two-body collisions with atoms and molecules. Although aspects of these interactions have been studied in detail [2,3], many unanswered questions remain which have relevance to fields such as atomic physics and surface science, as well as technological applications such as mass spectrometry. One area where there is relatively little direct experimental information is the interaction of positrons with atoms and molecules at low energies (e.g., <1 eV). Except for measurements of total cross sections [2,3], virtually all studies of positron-atom and positron-molecule scattering have concentrated on energies greater than a few electron volts. The lowest energy positron differential cross-section $d\sigma/d\Omega$ (DCS) measurement was for argon at 2.2 eV [8], and the only other total vibrational cross-section measurement we are aware of was for CO_2 at energies above 3 eV [7]. Current scientific questions of interest involving low-energy positrons include the possibility of bound states of positrons with atoms and molecules and the role of vibrational excitation in the formation of long-lived positron-molecule resonances and fragmentation following positron annihilation [5].

Progress in low-energy positron scattering has been hindered by limitations in available positron beam sources. Typical available positron sources have relatively large energy spreads of a few tenths of an electron volt, which prohibits beam experiments at low energy. Techniques used for producing narrow energy spread in electron beams, e.g., energy filtering copious electron sources, are not applicable to positron sources because they are wasteful of the scarce positron resource. We have been able to overcome these limitations using a novel technique that we recently developed for producing a high-intensity, cold, magnetized positron beam [9]. Using this cold beam, we have measured the DCS for positron collisions with Ar and Kr at energies below any previous measurements. We have also made the first low-energy measurements of vibrational excitation of molecules by positrons, studying the excitation of CF_4 at positron energies as low as 0.2 eV. This technique opens up a new and interesting energy regime to positron experiments.

Scattering experiments of this type have been traditionally carried out using electrostatic beams. Typically a highly compact target such as a gas jet is used to localize the scattering region, which in turn precisely defines the scattering angle [10]. By using the method described below to study charged particle scattering in a magnetized system, we have been able to replace the gas jet with a simple, differentially pumped scattering cell.

The experiment employs the cold magnetized positron beam line shown schematically in the upper panel of Fig. 1. Moderated positrons are accumulated from a radioactive source (not shown) in a specially designed Penning-Malmberg trap by means of inelastic collisions with a nitrogen buffer gas [11,12]. The positrons, which are accumulated at a rate of $\sim 1 \times 10^6$ e^+ s^{-1}, are confined radially by the magnetic field and axially by an electrostatic potential well (see the lower panel of Fig. 1). Once the positrons are trapped, they thermalize to room temperature (0.025 eV) by inelastic collisions with a nitrogen buffer gas [12]. A positron beam is then created by reducing the depth of the potential well confining the positrons, forcing them over a potential barrier E_0, which determines the beam energy. The positron beam is guided by the magnetic field through the differentially pumped
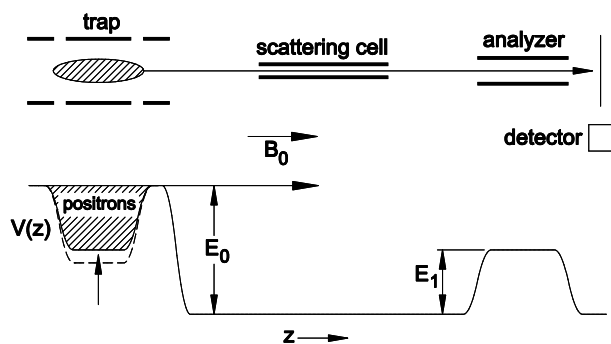

FIG. 1. (above) Schematic diagram of the scattering experiment showing the positron trap, scattering cell, and analyzer. (below) Plot of the potential profile $V(z)$ used to form and measure a scattered positron beam. As the depth of the potential well is reduced, positrons are forced over the potential barrier creating a positron beam at energy E_0 and analyzed using the retarding voltage E_1.

0031-9007/99/82(25)/5032(4)$15.00

scattering cell to the cylindrical retarding-potential energy analyzer. The beam energy is measured using a NaI(Tl) γ-ray detector to record the number of positrons which pass through the energy analyzer as a function of the retarding voltage E_1. A typical beam energy spread is 0.018 eV FWHM, with a beam energy range from ~ 0.1 to several tens of electron volts [9].

The scattering experiments are conducted using the following sequence. After the positrons are accumulated and cooled to room temperature, the nitrogen buffer gas is pumped out and a test gas is introduced into the center of the scattering cell. This cell consists of a 55 cm long, 1.2 cm diameter tube which is differentially pumped at both ends, so that the pressure drops by an order of magnitude from the center to the ends of the cell. The average pressure in the scattering cell ranged from 5×10^{-5} to 5×10^{-4} Torr and was adjusted to minimize the effects of multiple scattering. The absolute value of the test gas pressure was determined by extrapolating the pressure at the end of the scattering cell, which is measured by a stable-ion gauge with an absolute accuracy of 6%. To aid in the extrapolation, the pressure profile inside the scattering cell and elsewhere along the positron's path was calculated using a particle code. The cold positron beam, formed by the method described above, is passed through the cell, where $\approx 10\%$ of the positrons interact with the test gas. The energy distribution of the scattered beam is then measured using the retarding-potential analyzer. To improve the signal to noise ratio, the positron accumulation and beam dump cycle, which typically last 20 s, is repeated over 100 times for each energy scan.

All of our scattering measurements exploit the behavior of magnetized positrons in the 0.1 T magnetic field. We express the positron energy, E, as $E = E_\perp + E_\parallel$, where $E_\perp$ and $E_\parallel$ are the contributions to the energy due to motion perpendicular and parallel to the magnetic field. For the slowly changing fields employed in this experiment, the quantity $E_\perp / B$ is an adiabatic invariant. The effects of a scattering event on $E_\perp$ and $E_\parallel$ are shown in Fig. 2. When only elastic scattering is present, as is the case for the noble gases below the threshold for electronic excitation and positronium formation, the total energy E does not change as a result of the collision [see Fig. 2(b)]. Therefore, the scattering angle θ is determined solely by the value of $E_\parallel$ after a scattering event and is given by the relation $\theta = \cos^{-1}(\sqrt{E_\parallel / E})$.

Figure 3(a) shows the parallel energy distribution $I(E_\parallel)$, integrated over energies above $E_\parallel$, for a 1.05 eV positron beam scattered from Ar atoms. Using the integrated energy distribution $I(E_\parallel)$, the elastic DCS is obtained by $d\sigma/d\Omega = C\sqrt{EE_\parallel} \times dI(E_\parallel)/dE_\parallel$, where the constant of proportionality, C, depends on the gas cell pressure and length. This method was used previously by Coleman and McNutt, who measured $I(E_\parallel)$ using a time-of-flight technique; however, they were limited in the range of energies that they could study by the relatively large energy spread of their beam [8].
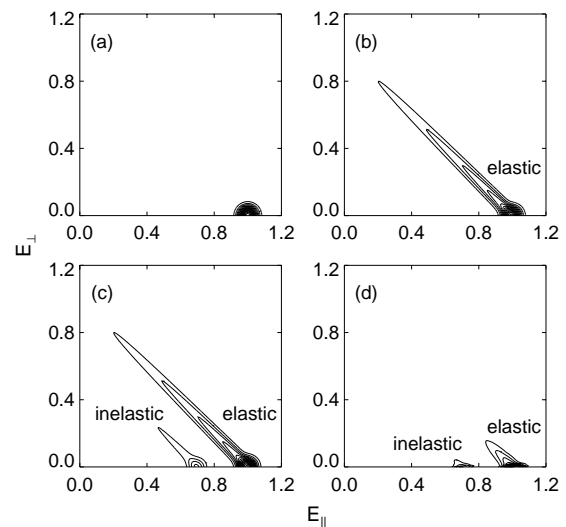

FIG. 2. Simulated data illustrating the effects of scattering on the parallel and perpendicular energy contributions of a strongly magnetized, cold charged particle beam: (a) incident beam; (b) the effect of elastic scattering; (c) both elastic and inelastic scattering; and (d) the scattered beam shown in (c), following an adiabatic reduction of the magnetic field by a factor of $M = 10$.

Using the method described above, we have been able to make DCS measurements for both Ar and Kr at energies ranging from 0.4 to 2.0 eV. In order to improve the signal to noise ratio, a three-point boxcar average was used on all data except the 0.4 eV argon measurement. Figures 4(a)–4(d) show absolute DCS measurements in atomic units for positron-argon scattering at energies of 0.4, 0.7, 1.0, and 1.5 eV, respectively. The DCS, in atomic units, are plotted versus the scattering angle folded around $\theta = \pi/2$, since the experiment simultaneously collects both back-scattered and forward-scattered particles. The solid line shows the predictions of a polarized orbital calculation [13] also
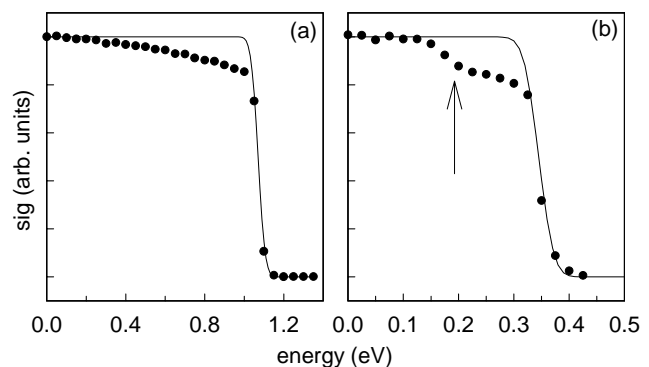

FIG. 3. Typical examples of raw data for the parallel energy distributions for elastic and inelastic scattering. ($\bullet$) Retarding-potential analyzer signal for (a) 1.05 eV positron beam after scattering off of Ar atoms; (b) 0.35 eV beam after scattering from CF_4. In (b), the arrow indicates the energy loss corresponding to the dominant vibrational mode (ν_3) in CF_4. The solid lines in both figures represent the transmitted beam when no gas is present.
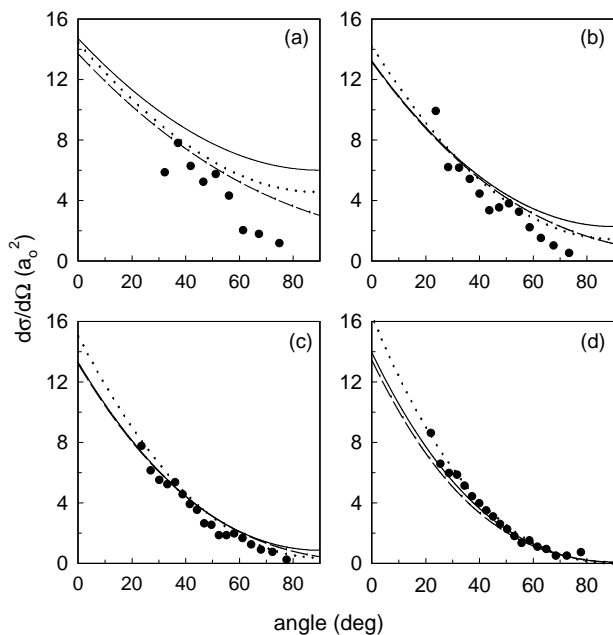
FIG. 4. Differential elastic cross sections for positron-argon scattering. Data for positron energies of 0.4, 0.7, 1.0, and 1.5 eV are shown in plots (a)–(d), respectively. Solid and dotted lines are the theoretical predictions of McEachran *et al.* [13] and Dzuba *et al.* [6], respectively, folded around $\theta = \pi/2$; dashed lines are the forward scattered contribution of McEachran's theory. There are no fitted parameters.

folded around $\theta = \pi/2$. The dashed line shows the same theory with only the forward-scattered component. The dotted line shows the predictions of a many-body theory by Dzuba *et al.* [6]. We have also measured the DCS for positron scattering from krypton, which has a total scattering cross section roughly twice that of argon. Figures 5(a) and 5(b) show a similar set of data for positron scattering from krypton at scattering energies of 1.0 and 2.0 eV. For both the argon and krypton elastic DCS measurements, experiment and theory are in reasonably good absolute agreement over most of the range of energies and angles. There appears to be systematic disagreement at large scattering angles and low energies which bears further scrutiny.

Using the cold beam, we have also measured the total vibrational cross section for CF_4 at positron beam energies from 0.2 to 0.9 eV. We are able to measure the energy lost in an inelastic collision by taking advantage of the adiabatic invariant, $E_\perp/B$. If the positron travels into a region where the magnetic field is reduced by a factor of M following a collision, then $E_\perp$ is reduced by the same factor while the total energy of the scattered positron remains constant. For a large reduction in field ($M \gg 1$), the resulting parallel energy $E_\parallel$ is approximately the total positron energy E [see Figs. 2(c) and 2(d)].

Figure 3(b) shows the parallel beam energy distribution, $E_\parallel$, for a 0.35 eV positron beam scattered from CF_4. A magnetic field ratio, $M = 3$, between the gas cell and the analyzer was used to increase the separation in $E_\parallel$ between elastic and inelastic scattering events.
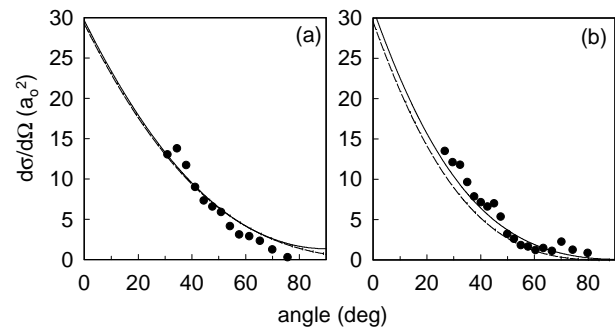
FIG. 5. Differential elastic cross sections for positron-krypton scattering at energies of (a) 1.0 and (b) 2.0 eV. Solid lines are the theoretical predictions of McEachran *et al.* [14], folded around $\theta = \pi/2$; dashed lines are the forward scattered contribution only. There are no fitted parameters.

The solid line depicts the transmitted beam as a function of retarding-potential energy without any scattering. The solid circles show the integrated parallel beam energy distribution after scattering from CF_4. The excitation of a vibrational mode in CF_4 is shown by a loss of positron energy as indicated by the arrow. We identify this energy loss to be due to the dominant asymmetric stretch mode ν_3 (0.157 eV) that is observed in electron scattering and infrared absorption experiments [15,16]. The inelastic scattering cross section is determined from Fig. 3(b) by measuring the size of the scattered component relative to that of the incident beam and normalizing according to the pressure in the scattering cell.

Figure 6 shows the inelastic cross section as a function of beam energy for positron and electron collisions with CF_4. We compare our data with the only available electron vibrational cross-section measurements for CF_4, which were obtained using the swarm technique [16]. While the electron cross section peaks above the ν_3 threshold (0.0157 eV), the positron data is qualitatively different, raising potentially interesting theoretical questions. Although there is theoretical work on the excitation of vibrational modes in molecules by positrons [7,17], to our knowledge there are no theoretical predictions for positron
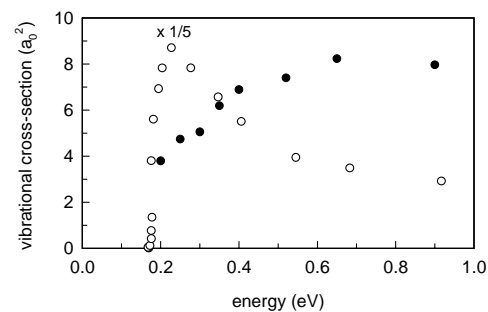

FIG. 6. Inelastic cross section shown as a function of energy for vibrational excitation of CF_4 by (●) positrons, and from (○) electron swarm data (Ref. [16] plotted at 1/5 actual value). The collisions with CF_4 excite the asymmetric stretch mode ν_3 at an energy of 0.157 eV.

scattering from CF_4. The only other measurements we are aware of for CF_4 are the total cross sections measured above 1 eV by Sueoka *et al.* [3].

We are now constructing a dedicated gas cell, located external to the trap, specifically designed for the scattering measurements described here. The magnetic field ratio, M, will be variable over a wider range, which should increase by about a factor of 10 the resolution of inelastic scattering measurements. We expect to be able to measure the full DCS when both elastic and inelastic scattering are present [18], by varying magnetic field ratio, M, and using tomographic reconstruction on the resulting two-dimensional data set in $E - M$ space to measure the DCS as a function of θ and E. Forward and back scattering will be resolved using a pulsed positron beam and time resolving the two components.

In conclusion, we have made the first low-energy measurements of the cross section for inelastic vibrational excitation of molecules with positrons, studying scattering from CF_4 at energies from 0.2 to 0.9 eV. We have also demonstrated that positron-atom DCS measurements are possible in an energy range below a few electron volts, which was not possible previously. There are a range of interesting problems that can now be addressed by this technique. For example, by studying the angular dependence of the elastic scattering at low energies, it should be possible to measure the sign and magnitude of the zero-energy scattering length, which determines the energies of low-lying virtual or weakly bound states. In the area of inelastic scattering, there are a number of interesting questions regarding the excitation of vibrational modes in molecules by positrons which can now be addressed.

We would like to thank G. Gribakin for many insightful conversations and for providing the theoretical curves shown in Figs. 4 and 5, and E. A. Jerzewski for technical assistance.

*Present address: First Point Scientific, Inc., 5330 Derry Ave., Suite J, Agoura Hills, CA 91360.

[1] P. J. Schultz and K. G. Lynn, Rev. Mod. Phys. **60**, 701 (1988).

[2] W. E. Kauppila and T. S. Stein, Adv. At. Mol. Opt. Phys. **26**, 1 (1990).

[3] O. Sueoka and A. Hamada, J. Phys. Soc. Jpn. **62**, 2669 (1993).

[4] M. Charlton and G. Laricchia, J. Phys. B **23**, 1045 (1990).

[5] K. Iwata *et al.,* Phys. Rev. A **51**, 473 (1995).

[6] V. A. Dzuba *et al.,* J. Phys. B **29**, 3151 (1996).

[7] M. Kimura *et al.,* Phys. Rev. Lett. **80**, 3936 (1998).

[8] P. G. Coleman and J. McNutt, Phys. Rev. Lett. **42**, 1130 (1979).

[9] S. J. Gilbert, C. Kurz, R. G. Greaves, and C. M. Surko, Appl. Phys. Lett. **70**, 1944 (1997); C. Kurz *et al.,* Nucl. Instrum. Methods Phys. Res., Sect. B **143**, 188 (1998).

[10] S. J. Buckman *et al.,* Meas. Sci. Technol. **4**, 1143 (1993).

[11] C. M. Surko, M. Leventhal, and A. Passner, Phys. Rev. Lett. **62**, 901 (1989).

[12] R. G. Greaves, M. D. Tinkle, and C. M. Surko, Phys. Plasmas **1**, 1439 (1994).

[13] R. P. McEachran *et al.,* J. Phys. B **12**, 1031 (1979).

[14] R. P. McEachran *et al.,* J. Phys. B **13**, 1281 (1980).

[15] A. Mann and F. Linder, J. Phys. B **25**, 533 (1992).

[16] L. G. Christophorou *et al.,* J. Phys. Chem. Ref. Data **25**, 1341 (1996).

[17] G. Danby and J. Tennyson, J. Phys. B **24**, 3517 (1991); F. A. Gianturco and T. Mukherjee, J. Phys. B **30**, 3567 (1997); P. Baille and J. W. Darewych, J. Phys. (Paris), Lett. **35**, 243 (1974).

[18] D. Boyd *et al.,* Phys. Lett. **45A**, 421 (1973).